



OPEN

Counts of hyaluronic acid-containing extracellular vesicles decrease in naturally occurring equine osteoarthritis

Anne-Mari Mustonen^{1,2✉}, Nina Lehmonen³, Sanna Oikari¹, Janne Capra⁴, Marja Raekallio³, Anna Mykkänen³, Tommi Paakkonen¹, Kirsi Rilla¹, Tytti Niemelä³ & Petteri Nieminen¹

Osteoarthritis (OA) is a degenerative joint disease with inadequately understood pathogenesis leading to pain and functional limitations. Extracellular vesicles (EVs) released by synovial joint cells can induce both pro- and anti-OA effects. Hyaluronic acid (HA) lubricates the surfaces of articular cartilage and is one of the bioactive molecules transported by EVs. In humans, altered EV counts and composition can be observed in OA synovial fluid (SF), while EV research is in early stages in the horse—a well-recognized OA model. The aim was to characterize SF EVs and their HA cargo in 19 horses. SF was collected after euthanasia from control, OA, and contralateral metacarpophalangeal joints. The SF HA concentrations and size distribution were determined with a sandwich-type enzyme-linked sorbent assay and size-exclusion chromatography. Ultracentrifugation followed by nanoparticle tracking analysis (NTA) were utilized to quantify small EVs, while confocal laser scanning microscopy (CLSM) and image analysis characterized larger EVs. The number and size distribution of small EVs measured by NTA were unaffected by OA, but these results may be limited by the lack of hyaluronidase pre-treatment of the samples. When visualized by CLSM, the number and proportion of larger HA-containing EVs (HA-EVs) decreased in OA SF (generalized linear model, count: $p = 0.024$, %: $p = 0.028$). There was an inverse association between the OA grade and total EV count, HA-EV count, and HA-EV % ($r_s = -0.264$ to -0.327 , $p = 0.012$ – 0.045). The total HA concentrations were also lower in OA (generalized linear model, $p = 0.002$). To conclude, the present study discovered a potential SF biomarker (HA-EVs) for naturally occurring equine OA. The roles of HA-EVs in the pathogenesis of OA and their potential as a joint disease biomarker and therapeutic target warrant future studies.

Abbreviations

AB	Apoptotic body
BM	Body mass
CD44	Cluster of differentiation 44
CL	Contralateral
CLSM	Confocal laser scanning microscopy
ELSA	Enzyme-linked sorbent assay
EV	Extracellular vesicle
EXO	Exosome
FLS	Fibroblast-like synoviocyte
GLM	Generalized linear model
HA	Hyaluronan
HABC	Hyaluronan binding complex
HA-EV	Hyaluronan-containing extracellular vesicle

¹Faculty of Health Sciences, School of Medicine, Institute of Biomedicine, University of Eastern Finland, P.O. Box 1627, 70211 Kuopio, Finland. ²Department of Environmental and Biological Sciences, Faculty of Science and Forestry, University of Eastern Finland, P.O. Box 111, 80101 Joensuu, Finland. ³Department of Equine and Small Animal Medicine, Faculty of Veterinary Medicine, University of Helsinki, P.O. Box 57, 00014 Helsinki, Finland. ⁴Cell and Tissue Imaging Unit, Faculty of Health Sciences, School of Medicine, Institute of Biomedicine, University of Eastern Finland, P.O. Box 1627, 70211 Kuopio, Finland. ✉email: anne-mari.mustonen@uef.fi

MV	Microvesicle
MSC	Mesenchymal stem cell
NSAID	Nonsteroidal anti-inflammatory drug
NTA	Nanoparticle tracking analysis
OA	Osteoarthritis
PBS	Phosphate buffered saline
RA	Rheumatoid arthritis
r_s	Spearman correlation coefficient
SDS	Sodium dodecyl sulphate
SEC	Size-exclusion chromatography
SF	Synovial fluid

Lameness is a major factor leading to poor performance and early retirement of equine athletes, and osteoarthritis (OA) is among its most common causes¹. Similar to the human condition, equine OA is a multifactorial degenerative disease affecting the whole joint². It is characterized by the destruction of articular cartilage and alterations in the subchondral bone and soft tissues of the joint, leading to pain and functional limitations¹. Joints affected by OA include, for instance, carpal, metacarpophalangeal, proximal/distal interphalangeal, carpometacarpal, tarsal, and femorotibial joints³. Prior trauma to the joint, immobilization, poor conformation, improper shoeing, and aging can contribute to the development of OA¹, which may occur early in the life of equine athletes or later in horses having less intensive exercise². Molecules that are associated with OA and/or experimentally-induced synovitis in horses include cytokines, other inflammatory mediators (e.g., chemokines, prostaglandin E₂, nitric oxide), and cartilage-degrading proteinases^{1,4}.

The currently available medical treatment for OA mostly offers symptomatic relief but fails to repair cartilage damage that is already present⁵. For this reason, early diagnosis before substantial joint pathology would be pivotal, and specific and sensitive biomarkers are actively sought for early-stage OA. Similar to humans, equine OA can occur spontaneously or post-traumatically⁶. Among existing animal models, equine (stifle) articular cartilage shows much promise, as its average thickness, cellular structure, as well as biochemical makeup and properties exhibit the most similarity to human cartilage. The possibility of repeated collection of substantial amounts of synovial fluid (SF) also makes the horse an attractive model for translational OA research in addition to veterinary interest. Biomarkers for equine OA are actively screened⁷ and, regarding SF, pro-inflammatory cytokines, chemokines, cartilage degeneration markers^{4,8}, proteomics⁹, eicosanoids¹⁰, extracellular vesicles (EVs), EV phospholipids¹¹, and EV small non-coding RNAs¹² have emerged as candidates for OA or synovitis, but reliable and easily accessible analyses to detect and monitor equine OA are still lacking.

EVs are nano- and micro-sized membrane-bound particles released by virtually all cell types in physiological and pathological conditions⁵. They constitute a heterogeneous mixture of subpopulations with different size and biogenesis (exosomes EXOs, microvesicles MVs, apoptotic bodies ABs, etc.). Here, the concept of EV is used as the collective term for all classes of cell-derived vesicles present in equine SF. EVs act as carriers of bioactive molecules and they can modulate the gene expression patterns and behaviour of target cells. Fibroblast-like synoviocytes (FLSs) play a central role in inflammation and cartilage degradation in joint diseases, and EVs have recently emerged as potential conveyors of these effects. SF EVs from arthritic patients can induce pro-inflammatory and catabolic effects on FLSs and chondrocytes but EVs, especially those from mesenchymal stem cells (MSCs), can also provide with anti-OA influence. FLSs are known to secrete EVs that transport hyaluronan (HA) cargo (HA-EVs)¹³. HA is a major glycosaminoglycan constituent of SF produced by FLSs¹⁴. It provides boundary lubrication, and its SF concentration and molecular size decrease in arthritic patients¹⁵.

The roles of HA-EVs have not been in the focus of OA research on horses, while SF EV counts increased in experimentally-induced synovitis, and especially the levels of cluster of differentiation 44 (CD44)-positive EVs were elevated in horse SF¹¹. Regarding EV lipidomics, short-chain carboxylic acid *N*-modified phosphatidylserine molecules may be involved in synovitis. When chondrocytes were incubated with SF EVs, there was downregulation of genes involved in joint inflammation¹¹, and by using EVs from equine bone marrow MSCs, the expression of cartilage-degrading proteinases could decrease in chondrocytes^{16,17}. EVs from horse amniotic mesenchymal-derived cells contain miRNAs that have potential effects, for instance, on interleukin signaling and inflammatory processes¹⁸. Data on the effects of OA on HA concentrations are variable in horses with unchanged or reduced HA levels and stable or impaired viscoelastic properties of OA SF^{19,20}. HA treatments can have beneficial influence on the health of joint tissues, including chondroprotection and anti-inflammatory effects^{21,22}.

Alterations in the levels of SF HA and EVs may contribute to the pathogenesis of OA and have potential as joint disease biomarkers and therapeutic targets^{5,23}. Based on this, the aim of the present study was to characterize SF EVs and their HA cargo in the naturally occurring equine OA model. It was hypothesized that (i) SF EV counts would be elevated in OA, (ii) HA concentrations and molecular weight would reduce in OA SF, and (iii) HA-EV counts would decrease in OA SF compared to control joints.

Methods

Animals and sampling. Approximately 3–10 ml of SF was aspirated from arthritic metacarpophalangeal joints of 11 horses (Table 1) at the Veterinary Teaching Hospital, University of Helsinki, after medically-induced euthanasia because of OA or due to other diagnoses (spinal or dental pathology, back pain, puncture wound in hoof, leg injury, guttural pouch mycosis). The protocols included 0.1–0.2 mg/kg detomidine hydrochloride, 0.1–0.2 mg/kg butorphanol tartrate, 0.05–0.1 mg/kg midazolam, 2.2 mg/kg ketamine hydrochloride, and T-61 euthanasia solution. The OA diagnosis was based on *post-mortem* macroscopic findings on the joint surfaces (presence of wear lines, erosion of articular cartilage, osteophytes)²⁴ photographed and assessed by experienced

	Control	CL	OA
Standardbred, n		1	1
Warmblood, n	5	9	9
Finnhorse, n	2		1
Pony, n	1		
Mare, n	5	5	6
Gelding, n	3	5	5
Horses, n	8	10	11
Joints, n	10	10	11

Table 1. Breeds and gender of the sampled horses. CL = contralateral, OA = osteoarthritis.

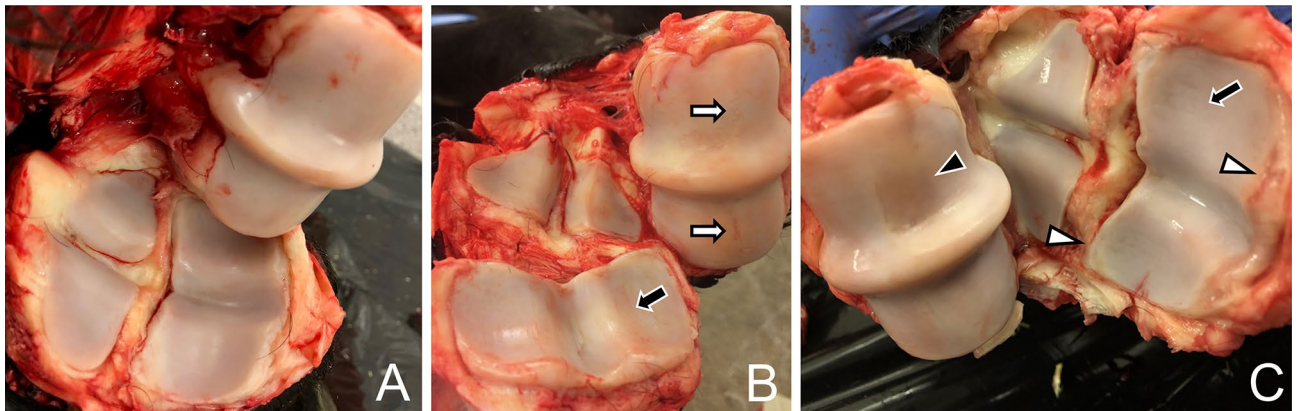


Figure 1. Representative photographs of articular cartilage in normal and osteoarthritic horse fetlock joints. A = normal, B = mild osteoarthritis (OA), C = severe OA, black arrows indicate thinning and wear lines in articular cartilage, white arrows indicate erosion, black arrowhead points to missing cartilage, and white arrowheads indicate osteophytosis.

equine veterinarians (Fig. 1). Contralateral (CL) fetlock joints were also sampled, and control samples were acquired from 7 age-matched horses and one pony (Table 1) euthanized for diagnoses other than OA (colic, sinusitis, wound, neurological disease, leg injury). In the *post-mortem* examination, the fetlock joint surfaces of control animals either had no macroscopic abnormalities or revealed mild periarticular changes.

The average age of the horses was 11 ± 1 years (range 4–20 years) and the body mass (BM) 518 ± 13 kg (400–600 kg). Information about the medication could not be retrieved for every individual, and 3 control and 3 CL/OA horses had been treated with nonsteroidal anti-inflammatory drugs (NSAIDs). In addition, 1 control and 2 CL/OA horses had received antibiotics and 1 CL/OA horse had been treated with antifungals. The joints were classified into diagnosis groups including control ($n = 7-8$ depending on analysis), CL ($n = 9-10$), and OA ($n = 9-10$) based on the *post-mortem* examination of the joint surfaces. As most CL joints were noted to have mild OA, the joints were also scored according to OA severity as follows: 0 = normal ($n = 6-8$), 1 = mild OA ($n = 8$), 2 = moderate OA ($n = 4-5$), and 3 = severe OA ($n = 7-8$). The SF samples were immediately frozen in liquid nitrogen and stored at -80 °C until analyzed.

Nanoparticle tracking analysis (NTA). For NTA, SF samples (1 ml, $n = 26$) were processed as follows: centrifugation at $1000 \times g$ for 10 min, centrifugation of the supernatant at $2000 \times g$ for 20 min, ultracentrifugation of the supernatant at $110,000 \times g$ for 2 h and again for 90 min to wash the pellet, followed by its resuspension in $100 \mu\text{l}$ of $0.1 \mu\text{m}$ -filtered phosphate buffered saline (PBS). The Optima LE-80 K ultracentrifuge with the Ti 50.2 rotor and k-factor of 143.3 (Beckman Coulter, Brea, CA, USA) was used for ultracentrifugation.

These enriched EV samples were analyzed by NTA using the NanoSight model LM14 (Malvern Panalytical, Malvern, UK) equipped with blue laser (404 nm, 70 mW) and the sCMOS camera (Hamamatsu Photonics, Hamamatsu, Japan). The samples were diluted in $0.1 \mu\text{m}$ -filtered PBS to obtain 40–100 particles/view, and five 30-s videos were recorded using camera level 14. The data were analyzed using the NTA software v3.0 with the detection threshold 5 to track as many particles as possible with minimal background. After the first analysis, the samples were treated with sodium dodecyl sulphate (SDS) to lyse the EVs²⁵ and re-run allowing the estimation of the proportion of EVs in the total particle counts¹³.

Confocal laser scanning microscopy (CLSM). The visualization of SF EVs with CLSM was performed as described previously²⁶. In brief, the plasma membranes of EVs were stained with CellMask Deep Red plasma

membrane stain (Thermo Fisher Scientific, Waltham, MA, USA) that was soluted together with Alexa Fluor 568-labeled HA binding complex (HABC) to visualize HA²⁷. Phalloidin-iFluor, conjugated to Alexa Fluor 594 (Abcam, Cambridge, UK), was used to validate the visualized structures as actual EVs. CellMask and HABC stainings were first performed on unprocessed SFs ($n = 29$), and then on the same samples centrifuged at $1000 \times g$ for 10 min to deplete any cell fragments. For phalloidin staining, SF was (ultra)centrifuged ($1000 \times g$ for 10 min, $1200 \times g$ for 20 min, $< 110,000 \times g$ for 90 min), and the ibidi coverglass the EV fraction was placed on was coated with poly-D-lysine hydrobromide. The Zeiss Axio Observer inverted microscope equipped with the Zeiss LSM 800 confocal module was used for imaging, and the initial image acquisition was carried out using the ZEN 2.3 blue edition software (Carl Zeiss MicroImaging GmbH, Jena, Germany). The area and intensity of the stainings, particle counts, and their size distribution were determined with the ImageJ/Fiji software (NIH, Bethesda, MA) as outlined previously²⁶.

HA determinations. The total HA concentration in SFs ($n = 26$) was determined with a sandwich-type enzyme-linked sorbent assay (ELSA) and the HA molecular weight distribution with size-exclusion chromatography (SEC), as described previously with slight modifications²⁶.

Statistical analyses. The power analysis was conducted using the IBM SPSS v27.0 program (IBM, Armonk, NY, USA) with the Bonferroni correction for the estimation of statistical power separately for the general variables, NTA, CLSM, and HA data. The obtained power values varied between 0.954 and 1.000, all well above the conventional limit for reliable testing to avoid type II errors, 0.8. Comparisons between the study groups were performed with the generalized linear model (GLM), and the sex ratios were tested with the Fisher's exact test (IBM SPSS v25.0 software). Correlations with OA grading were calculated with the Spearman correlation coefficient (r_s). The p value < 0.05 was considered statistically significant. The results were presented as the mean \pm SE. The discriminant analysis was performed separately for the different data types (NTA, CLSM, and HA data) to assess how clearly the samples in the study groups differed from one another, which variables separated them most clearly, and how well the analysis was able to classify the samples into their respective diagnoses.

Ethics approval. Informed owner consent was obtained for each horse, and ethical approval was provided by the Viikki Campus Research Ethics Committee of the University of Helsinki (Statement 1/2018).

Results

General variables. There were no statistically significant differences between the ages or sex distribution according to diagnosis group or OA grade (GLM, Fisher's exact test, $p > 0.05$). The average BMs were higher in CL/OA horses compared to controls (544 ± 12 vs. 492 ± 22 kg; GLM, $p = 0.023$), and this was also observed for grade 1 OA (541 ± 12 kg) and grade 3 OA (544 ± 14 kg) vs. grade 0 OA (481 ± 25 kg; $p = 0.017$). The CL joints showed significantly lower scores in OA grading (1.2 ± 0.20) than the OA joints (2.8 ± 0.13 ; GLM, $p < 0.001$).

Count and size distribution of small EVs in horse SF. The total particle count averaged $12.0 \times 10^{10} \pm 3.28 \times 10^{10}$ particles/ml in horse SF by NTA (Fig. 2A). After the detergent treatment, it was observed that most of these particles were non-vesicular material and the estimated concentration of EVs was $1.8 \times 10^{10} \pm 0.32 \times 10^{10}$ particles/ml. The majority of the particles were 100–200 nm in diameter, and there were no statistically significant differences in their count, diameter, or size distribution according to diagnosis or OA severity (GLM, $p > 0.05$; Fig. 2A–C). The discriminant analysis classified 87.5% of the samples correctly into their respective diagnosis groups based on the NTA data, and the discriminant functions 1–2 explained 100% of the variation in the dataset.

Count and size distribution of large EVs in horse SF. CLSM verified that the horse SF samples contained spherical EVs and that HA and phalloidin (a marker of filamentous actin) were co-localized with the plasma membrane stain (Fig. 3). With CLSM, we documented an EV population, the diameter of which was mostly < 1000 – 2000 nm, while the visualized HA-particles averaged < 1000 nm in diameter. The size distributions of both EVs and HA-particles were generally similar in all diagnosis groups (GLM, $p > 0.05$). Centrifugation of SF at $1000 \times g$ for 10 min caused decreases in the area, diameter, and intensity of membrane-fluorescent material (*i.e.*, EVs), co-localization of EV and HA fluorescences, and HA–EV count ($p = 0.011$ – 0.041).

In respect to diagnosis group, EV diameter was higher in OA SF (1575 ± 56 nm) compared to control SF (1402 ± 34 nm; GLM, $p = 0.034$). Approximately $10.4 \pm 1.09\%$ of EV fluorescence was co-localized with HA fluorescence. HA–EV count and % were lower in CL and OA SFs than in control SF ($p = 0.024$ – 0.028 ; Fig. 4A–B). HA–EV count also decreased in grade 3 OA compared to grade 0 samples ($p = 0.012$). There were no differences in EV or HA counts, areas of EVs or HA-particles, intensities of EV or HA fluorescences, HA-particle diameter, and area or diameter of HA–EVs ($p > 0.05$). There was an inverse correlation between OA grade and EV count, HA–EV count, and HA–EV % ($r_s = -0.264$ to -0.327 , $p = 0.012$ – 0.045). The association was positive for EV area and EV diameter with OA grade ($r_s = 0.272$, $p = 0.039$ for both).

For the discriminant analysis, the SF samples were divided into 6 subgroups (3 diagnoses with or without centrifugation) but neither diagnosis nor processing led to a separation of the samples into discrete clusters (Fig. 5). The variables of interest contributing to the model included HA–EV count and HA–EV %. The functions 1–5 explained 100% of the variance in the dataset, and the analysis classified 71.2% of the samples correctly into their respective diagnosis groups.

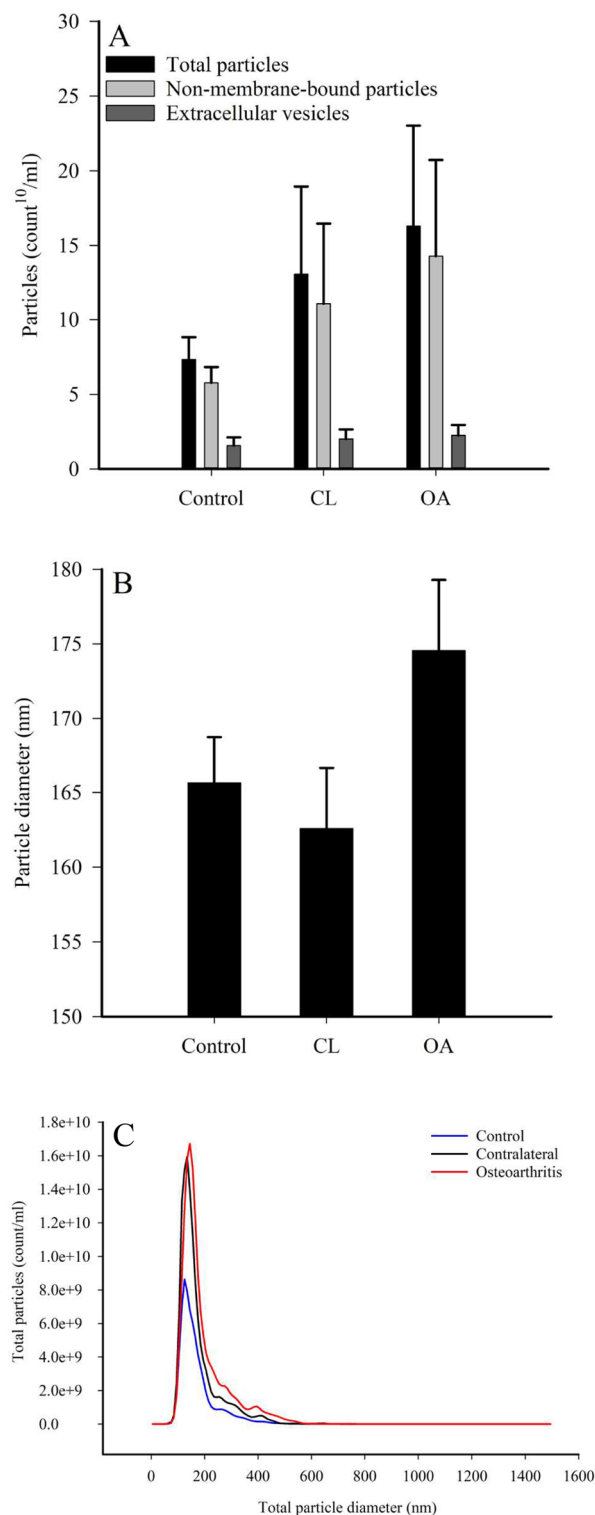


Figure 2. Particle counts (A), diameters of total particles (B), and size distribution of total particles (C) in equine synovial fluids. The samples were collected from control, contralateral (CL), and osteoarthritic (OA) fetlock joints and measured by nanoparticle tracking analysis (means + SE or means). There were no statistically significant differences between the groups (generalized linear model, $p > 0.05$).

HA concentrations in SF. The total HA concentrations were lower in CL and OA joints compared to controls (GLM, $p = 0.002$; Fig. 6A) and in OA grades 1–3 compared to grade 0 ($p = 0.021$). The size distribution of

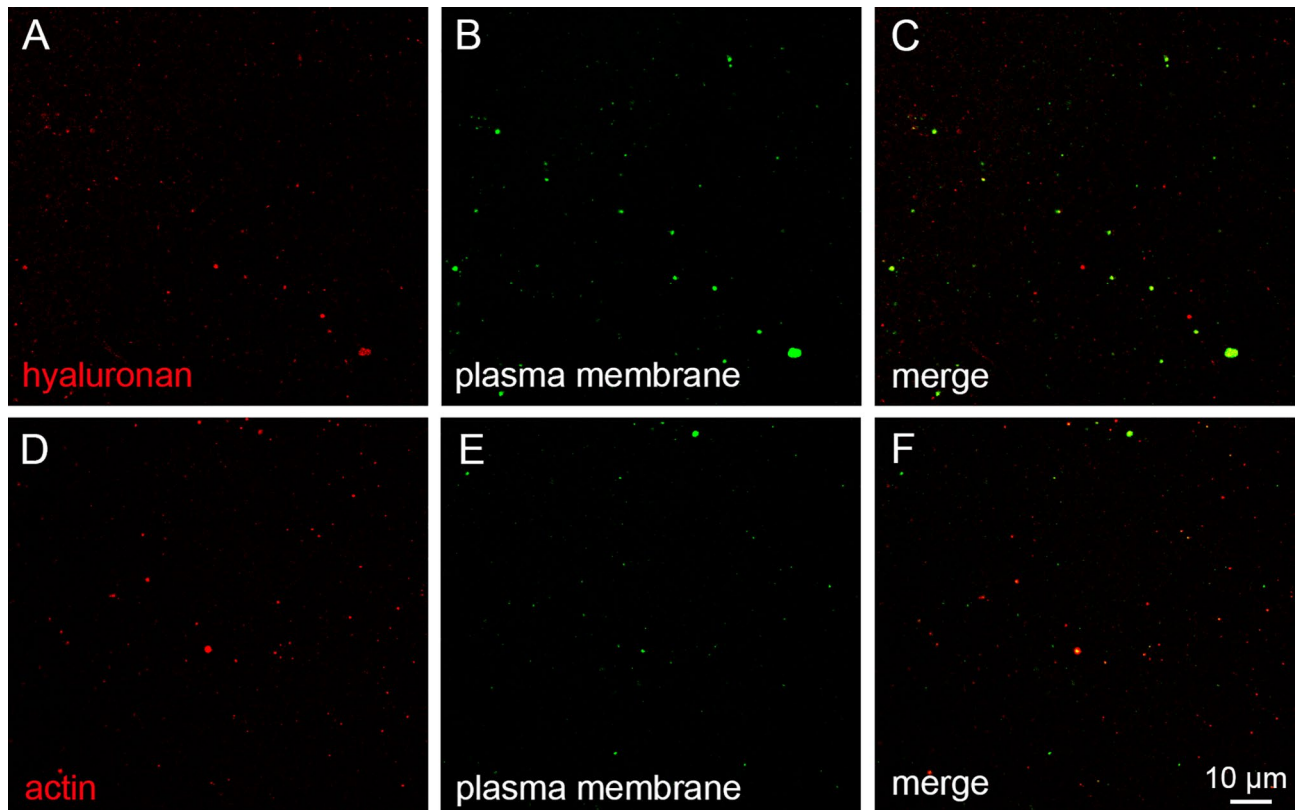


Figure 3. Equine synovial fluid (SF) stained with CellMask Deep Red plasma membrane stain, Alexa Fluor 568-labeled hyaluronan binding complex (HABC), and Alexa Fluor 594-labeled phalloidin. An unprocessed SF sample stained with HABC (pseudocolored red) and CellMask (pseudocolored green) in panels (A and B), an ultracentrifuged SF sample stained with phalloidin (pseudocolored red) and CellMask (pseudocolored green) in panels (D and E), and merged images in panels (C and F) depicting the co-localization of the stains.

HA fractions with different molecular weights was mostly similar in all diagnosis groups and, on average, > 90% of HA was of high molecular weight (≈ 2500 kDa; Fig. 6B).

In the discriminant analysis, control joints were clearly separated from CL and OA joints that partly clustered together based on the HA data (Fig. 6C). The total HA concentration ($\mu\text{g}/\text{ml}$) was more pivotal for the separation of the groups than the fractions with different molecular weights. The first function explained 95.1% of the variance in the dataset and the second function accounted for 4.9% of the variance. The analysis classified 92.0% of the samples correctly into their respective diagnosis groups.

Discussion

In the present study, we characterized SF EV populations and determined HA levels in the naturally occurring equine OA model by various methods (NTA, CLSM, ELSA, and SEC). CLSM verified that the SF samples contained spherical membrane-coated particles with filamentous actin, a cytosolic protein recovered in EVs²⁸. The main findings were as follows: (i) the number and size distribution of small EVs measured by NTA were unaffected by OA, (ii) larger EVs determined by CLSM increased in size but tended to decrease in number due to OA, (iii) the number and proportion of HA–EVs decreased in OA SF, (iv) total HA concentrations reduced in OA SF, and (v) CL joints with milder OA resembled OA joints in their EV and HA data.

Leukocytes and FLSs are among cellular sources of SF EVs, the quantity and composition of which can be altered in human patients with OA and rheumatoid arthritis (RA)^{5,29}. In the present study using equine SF, the average counts and diameters of total particles detected by NTA were not affected by OA. Generally speaking, simply using NTA results as diagnostic or prognostic tools would be inadequate. This is due to methodological limitations, as NTA cannot distinguish EVs from non-membrane-bound particles³⁰, which would cause a confounding factor in the analysis. In fact, the treatment of the ultracentrifuged fraction with SDS demonstrated that most of the detected particles did not represent vesicular structures. The diameter of membrane-bound particles was mostly > 100 nm in our preparation suggesting that this EV population mainly consisted of MVs. Previous studies have reported increases in cytokine- and chemokine-rich EXOs from early to severe knee OA³¹ or no differences in EV concentrations between the SFs of OA and non-OA human patients³². Research on EVs in equine OA SF is still in its early stages, but their counts, especially those with CD44, increased in experimentally-induced synovitis¹¹. This was different from the unaffected counts of small EVs in our naturally occurring OA model, emphasizing the need for both model types in horse EV research. It would be possible to

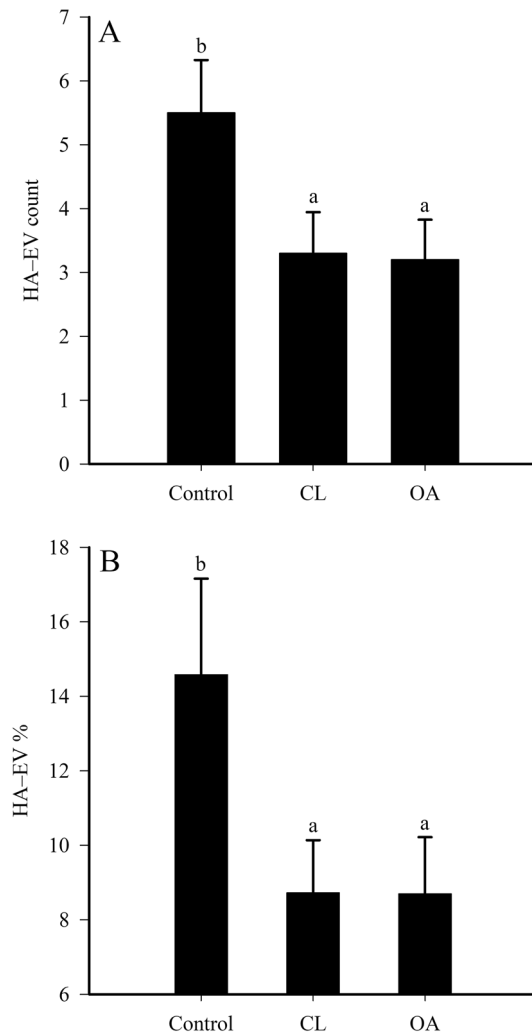


Figure 4. Count (A) and % (B) of hyaluronan-containing extracellular vesicles (HA-EVs) in equine synovial fluids. The samples were collected from control, contralateral (CL), and osteoarthritic (OA) fetlock joints (means + SE). HA-EV % represents the proportion of EVs with HA staining of the total EV count on the visual fields. Bars with dissimilar lowercase letters differ significantly from each other (generalized linear model, $p < 0.05$).

optimize the EV recovery from equine SF by pre-treatment of samples with hyaluronidase¹¹, the lack of which may have reduced the counts of especially CD44⁺ EVs in the present study.

A large proportion of previous studies has focused on EXOs, but biofluids also contain other subpopulations of EVs that presumably have different characteristics and functional properties. According to Jimenez et al.³³, small EVs (EXOs) could promote cell adhesion, while larger EVs (MVs) were enriched in proteins associated with ribosomes, RNA biogenesis and processing, and metabolism. EVs with a diameter > 1000 nm have traditionally been considered ABs, but it is now known that they can also be produced by viable cells³⁴. The data on the cargo and function of these large EVs are scarce, as they are often routinely discarded by EV isolation techniques. However, human RA SF was documented to contain two subpopulations of EVs, small (100–300 nm) and large (700–3000 nm), the latter of which was associated with immune complexes³⁵. In the present study, we also observed a subpopulation of large EVs in equine SF by CLSM, and OA was noted to cause a slight increase in the average diameter of these EVs. There was also an inverse association between the EV number and OA grade. A change in particle size is not routinely observed due to OA^{31,32}, but Foers et al.²⁹ documented lower EV concentrations but higher diameters in OA SF compared to RA SF with high-level inflammation. In human patients with autoimmune systemic lupus erythematosus, plasma contained elevated levels of large EVs (700–3000 nm)³⁶ and, regarding horse plasma, endurance racing tended to increase the EV count and diameter³⁷. The reason for the observed slight increase in the EV size remains unknown but it could be speculated to be related to, for instance, elevated proportions of ABs in conditions with high inflammation or physical exercise.

The present study displayed reduced HA-EV counts and % in SF due to equine OA, which was not previously documented for human SF with the same CLSM technique²⁶. Different cell types can release HA-EVs but their functions remain unknown³⁸. They have been hypothesized to carry HA to distant sites, be able to synthesize

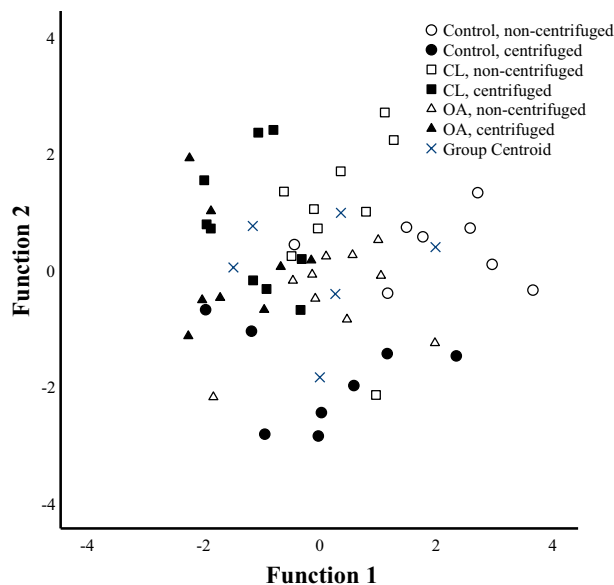


Figure 5. Discriminant analysis depicting the classification of confocal laser scanning microscopy data in equine synovial fluids. The samples were collected from control, contralateral (CL), and osteoarthritic (OA) fetlock joints, and the data classified based on discriminant functions 1 (on x-axis) and 2 (y-axis) that together explain 57.5% of the variance in the dataset. The samples were analyzed unprocessed and centrifuged at $1000\times g$ for 10 min prior to re-run.

new HA, transport signals to target cells, function in tissue remodeling and regeneration, and affect motility and metastasis of cancer cells. By transporting bioactive cargo, HA-EVs may also participate in inflammatory or pro-resolving processes in inflamed joints. In the present sample material, the proportion of HA-EVs of total EVs was approximately 12% in unprocessed SF and lower than measured previously in humans²⁶. If the reduction in the HA-EV counts could be shown to be a general feature of equine OA SF, HA-EVs may have potential as a joint disease biomarker and therapeutic target, as their levels can be monitored with CLSM by using simple stainings. The analysis does not require a great deal of post-sampling processing, but the access to specialized equipment would limit the applicability of HA-EVs as a biomarker. For translational studies, the factors modifying EV secretion in inflammation could be examined in the future and/or EV preparations could be given as therapeutic agents. It remains to be investigated if the reduction of HA cargo could justify the supplementation of HA in equine OA joints. Despite well-established beneficial effects, there is emerging controversy regarding the clinical effectiveness of intra-articular HA administrations³⁹. In fact, recent integration of meta-analysis with bioinformatics revealed that HA could also induce local and systemic inflammatory responses and may not be ultimately beneficial as an OA treatment.

Previously, when equine chondrocytes were incubated with SF EVs, genes involved in joint inflammation were downregulated, thus, implying anti-OA effects¹¹, and indications of decreased cartilage degradation by bone marrow MSC-derived EVs were documented in other recent horse studies^{16,17}. The present experiment observed a loss of HA-EVs in equine OA SF that is known to be of inflammatory nature⁸, but it remains to be established if HA-EVs would be beneficial for the joint health or if they could play a role in disease pathogenesis. EVs derived from inflammatory cells and chondrocytes can activate anabolic gene expression and reduce the expression of cartilage-degrading proteinases in chondrocytes, resulting in the deposition of extracellular matrix and cartilage protection^{40,41}. They can also polarize macrophage response towards an anti-inflammatory phenotype in cartilage and synovium and attenuate the development of experimentally-induced arthritis in animal models. Especially MSC-derived EVs can alleviate inflammation and pain as well as induce cartilage repair⁵. The potential roles HA-EVs could play in inflammation/resolution and degradation/repair in the joint environment should be investigated in future studies. Previous research has shown that intra-articular injections of high-molecular-weight HA combined with stem cell-derived EVs can improve cartilage repair and regeneration compared to HA alone⁴². The observations of the changes in HA-EVs in joint disease add to this knowledge and offer a new direction of EV research in OA of human and animal patients.

It was observed in the present study that the centrifugation of horse SF at $1000\times g$ for 10 min decreased the area, diameter, and intensity of EV fluorescence, co-localization of EV and HA fluorescences, and HA-EV count. While centrifugation is useful in removing larger particles, such as cellular debris, it also changes the characteristics of the desired research targets. Thus, it is of importance to examine not only processed samples but also biological fluids in their original state to gain comprehensive knowledge on EV biology. It was previously reported that the cellular origin of EVs can determine how they are affected by centrifugation and, for instance, the centrifugation of human plasma at $18,890\times g$ for 2 h at 20°C resulted in the aggregation of EVs⁴³. Our findings suggest that even low-speed centrifugation could influence the characteristics and cargo of EVs,

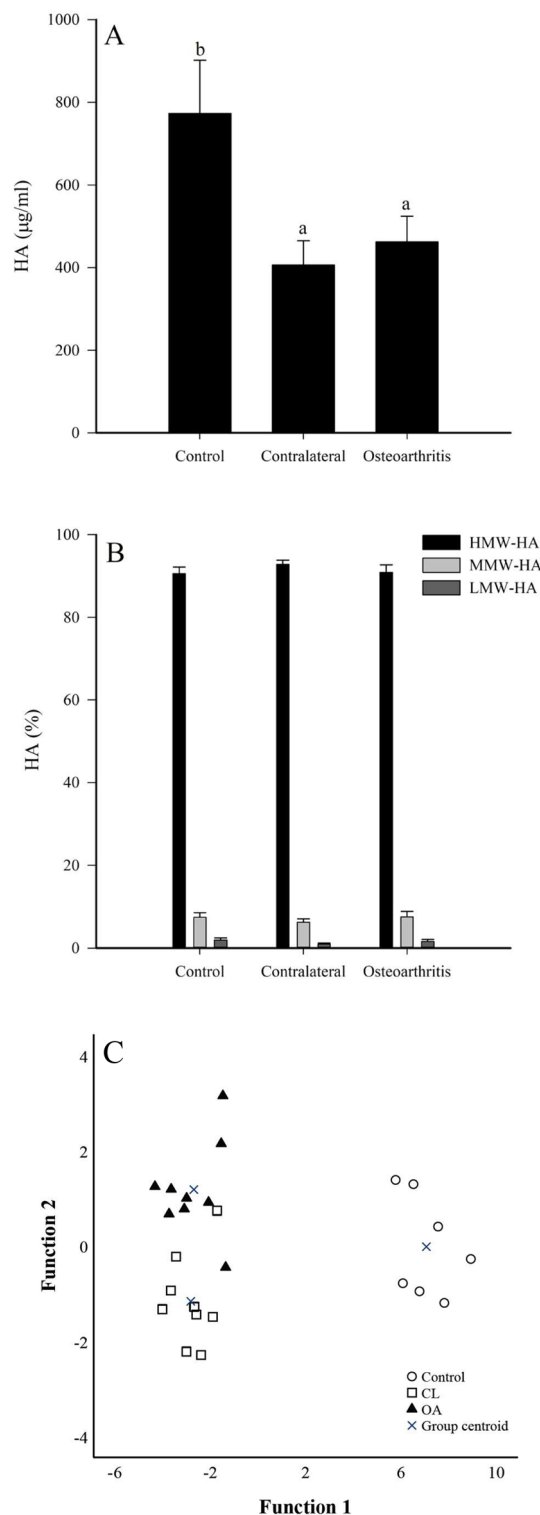


Figure 6. Total hyaluronan (HA) concentrations (A) and size distribution (B) in equine synovial fluids from control, contralateral (CL), and osteoarthritic (OA) fetlock joints (means + SE). Bars with dissimilar lowercase letters differ significantly from each other (generalized linear model, $p < 0.05$). Discriminant analysis (C) depicting the classification of HA data in equine synovial fluids based on discriminant functions 1 (on x-axis) and 2 (y-axis) that together explain 100% of the variance in the dataset. HMW = high-molecular-weight (≈ 2500 kDa), MMW = medium-molecular-weight (≈ 500 kDa), LMW = low-molecular-weight (≈ 150 kDa).

which highlights the need for careful reporting of all steps of EV sample processing. Furthermore, it is becoming clear that unprocessed, centrifuged, and ultracentrifuged samples reflect different particle populations in SF, and while different centrifugation protocols can assist in the visualization of smaller particles, the populations of larger EVs are either decreased or lost and, thus, their potential biological significance would remain uninvestigated. We tentatively suggest that it would be prudent to continue assessing various EV populations at this stage of equine EV research.

Regarding the conventional measurement of HA concentrations, the total HA levels decreased in both OA and CL SFs, while the molecular size distribution of HA remained unaffected. These results agree with previous data from OA horses with unchanged or decreased HA levels and stable or impaired viscoelastic properties of SF^{19,20}. HA is utilized in OA therapies of both human and equine patients, as it can induce chondroprotection and anti-inflammatory effects¹⁴. SF HA may also influence the uptake of EVs into joint tissues and, thus, mediate cell-to-cell communication. EVs have been shown to enter, for instance, synoviocytes, and the HA matrix around FLSS facilitates EV internalization, which may be partly mediated via CD44 on the EV surface⁴⁴. In fact, CD44⁺ EVs became elevated in the SF of horses with experimentally-induced synovitis¹¹.

The present study documented similarities in the EV and HA data between the CL and OA joints of horses. In studies using experimentally-induced OA models, CL knees are sometimes used as within-animal controls⁴⁵, but it is known that their biomechanical properties can be altered⁴⁶ and, in a rabbit model, several types of differences were documented in joint tissues between control and CL knees^{47–49}. For this reason, we expected that the characteristics of CL SF would differ from control joints, and the *post-mortem* examination of joint surfaces confirmed that mild OA was present in most of the CL joints²³. This emphasizes the need for a thorough examination of the CL joint, as it cannot be considered unaffected by the OA joint or be uncritically used for comparison as a control. It is well established in human studies that unilateral knee OA is a risk factor for developing bilateral knee OA⁵⁰. The grading scores of the CL joints were clearly lower than those of the OA joints, but they still exhibited the reduced HA–EV counts. This could provide future diagnostics and prognostics a useful tool to detect early-stage OA and to implement appropriate measures (such as level of exercise) to prevent further damage on the joint.

There are some limitations to be considered in the present study. The number of animals was relatively small, as it was difficult to obtain euthanized horses with unaffected fetlock joints. For this reason, one Estonian riding pony was included in the control group. Despite some variation in the assignment of the different breeds into the experimental groups, there was no statistical difference in their distribution. It was also impossible to determine if the diagnosed OA cases were spontaneous, of post-traumatic origin or, in one case, initiated by osteochondrosis. A few animals were euthanized for OA, while the remaining OA horses had only mild symptoms and OA was more of an incidental finding in these cases. Intra-articular medication was not administered to the animals, but 6 horses had been treated with NSAIDs, which may have influenced EV populations, albeit literature about the possible interactions between NSAID use and EV release remains scarce⁵¹. Finally, the SF samples were not pre-treated with hyaluronidase before ultracentrifugation, which could have reduced the recovery of especially CD44⁺ EVs for NTA¹¹.

Conclusion

The diagnosis of early OA still lacks specific molecular markers in body fluids for both humans and horses. The present study discovered a potential biomarker candidate for naturally occurring equine OA. The observed reduction in large HA–EVs could provide an additional tool for the diagnosis of early-stage OA before this debilitating condition becomes symptomatic or radiological signs develop. Eventually this would allow the development of early-stage measures to counteract the cartilage destruction that is the hallmark of inflammatory joint diseases. Based on the results of the present study, the association of HA–EVs with other related diseases also merits further research.

Data availability

All relevant data generated or analyzed during this study are included in this published article.

Received: 22 July 2022; Accepted: 27 September 2022

Published online: 20 October 2022

References

- Schlueter, A. E. & Orth, M. W. Equine osteoarthritis: A brief review of the disease and its causes. *Equine Comp. Exerc. Physiol.* **1**, 221–231 (2004).
- McIlwraith, C. W., Frisbie, D. D. & Kawcak, C. E. The horse as a model of naturally occurring osteoarthritis. *Bone Joint Res.* **1**, 297–309 (2012).
- Ross, M. W. Anamnesis (History). In *Diagnosis and management of lameness in the horse* 2nd edn (eds Ross, M. W. & Dyson, S. J.) 8–15 (Elsevier Saunders, Philadelphia, 2011).
- Watkins, A. *et al.* Investigation of synovial fluid lubricants and inflammatory cytokines in the horse: A comparison of recombinant interleukin 1 beta-induced synovitis and joint lavage models. *BMC Vet. Res.* **17**, 189 (2021).
- Mustonen, A.-M. & Nieminen, P. Extracellular vesicles and their potential significance in the pathogenesis and treatment of osteoarthritis. *Pharmaceuticals* **14**, 315 (2021).
- McCoy, A. M. Animal models of osteoarthritis: Comparisons and key considerations. *Vet. Pathol.* **52**, 803–818 (2015).
- McIlwraith, C. W. *et al.* Biomarkers for equine joint injury and osteoarthritis. *J. Orthop. Res.* **36**, 823–831 (2018).
- Bertuglia, A., Pagliara, E., Grego, E., Ricci, A. & Brkljaca-Bottegato, N. Pro-inflammatory cytokines and structural biomarkers are effective to categorize osteoarthritis phenotype and progression in Standardbred racehorses over five years of racing career. *BMC Vet. Res.* **12**, 246 (2016).
- Chiaradia, E. *et al.* Gambling on putative biomarkers of osteoarthritis and osteochondrosis by equine synovial fluid proteomics. *J. Proteomics* **75**, 4478–4493 (2012).

10. de Grauw, J. C., van de Lest, C. H. A. & van Weeren, P. R. A targeted lipidomics approach to the study of eicosanoid release in synovial joints. *Arthritis Res. Ther.* **13**, R123 (2011).
11. Boere, J. *Extracellular vesicles in synovial fluid: Dynamics during joint inflammation and articular development and promise for joint regeneration and restoration of joint homeostasis*. PhD Thesis, University Utrecht, the Netherlands (2017).
12. Anderson, J. R. *et al.* Small non-coding RNA landscape of extracellular vesicles from a post-traumatic model of equine osteoarthritis. *Front. Vet. Sci.* **9**, 901269 (2022).
13. Mustonen, A.-M. *et al.* First in vivo detection and characterization of hyaluronan-coated extracellular vesicles in human synovial fluid. *J. Orthop. Res.* **34**, 1960–1968 (2016).
14. Gupta, R. C., Lall, R., Srivastava, A. & Sinha, A. Hyaluronic acid: Molecular mechanisms and therapeutic trajectory. *Front. Vet. Sci.* **6**, 192 (2019).
15. Kosinska, M. K. *et al.* Articular joint lubricants during osteoarthritis and rheumatoid arthritis display altered levels and molecular species. *PLoS ONE* **10**, e0125192 (2015).
16. Arévalo-Turrubiarte, M., Baratta, M., Ponti, G., Chiaradia, E. & Martignani, E. Extracellular vesicles from equine mesenchymal stem cells decrease inflammation markers in chondrocytes *in vitro*. *Equine Vet. J.* <https://doi.org/10.1111/evj.13537> (2021).
17. Hotham, W. E., Thompson, C., Szu-Ting, L. & Henson, F. M. D. The anti-inflammatory effects of equine bone marrow stem cell-derived extracellular vesicles on autologous chondrocytes. *Vet. Rec. Open* **8**, e22 (2021).
18. Lange-Consiglio, A. *et al.* MicroRNAs of equine amniotic mesenchymal cell-derived microvesicles and their involvement in anti-inflammatory processes. *Cell Transplant.* **27**, 45–54 (2018).
19. Tyrnenopoulou, P. *et al.* Alterations in the viscoelastic properties of equine synovial fluid from fetlock joints with naturally occurring osteoarthritis. *Arch. Vetr. Sci. Med.* **1**, 1–9 (2020).
20. Matheson, A. *et al.* Proteoglycan-4 and hyaluronan composition in synovial fluid and serum from clinical equine subjects: Relationship to cartilage boundary lubrication and viscosity of synovial fluid. *Connect. Tissue Res.* **62**, 369–380 (2021).
21. Santangelo, K. S., Johnson, A. L., Ruppert, A. S. & Bertone, A. L. Effects of hyaluronan treatment on lipopolysaccharide-challenged fibroblast-like synovial cells. *Arthritis Res. Ther.* **9**, R1 (2007).
22. Neuenschwander, H. M. *et al.* Hyaluronic acid has chondroprotective and joint-preserving effects on LPS-induced synovitis in horses. *J. Vet. Sci.* **20**, e67 (2019).
23. Fuller, C. J., Barr, A. R., Sharif, M. & Dieppe, P. A. Cross-sectional comparison of synovial fluid biochemical markers in equine osteoarthritis and the correlation of these markers with articular cartilage damage. *Osteoarthr. Cartil.* **9**, 49–55 (2001).
24. McIlwraith, C. W. *et al.* The OARSI histopathology initiative – Recommendations for histological assessments of osteoarthritis in the horse. *Osteoarthr. Cartil.* **18**, S93–S105 (2010).
25. Osteikoetxea, X. *et al.* Differential detergent sensitivity of extracellular vesicle subpopulations. *Org. Biomol. Chem.* **13**, 9775–9782 (2015).
26. Mustonen, A.-M. *et al.* Characterization of hyaluronan-coated extracellular vesicles in synovial fluid of patients with osteoarthritis and rheumatoid arthritis. *BMC Musculoskelet. Disord.* **22**, 247 (2021).
27. Rilla, K., Tiuhonen, R., Kultti, A., Tammi, M. & Tammi, R. Pericellular hyaluronan coat visualized in live cells with a fluorescent probe is scaffolded by plasma membrane protrusions. *J. Histochem. Cytochem.* **56**, 901–910 (2008).
28. Théry, C. *et al.* Minimal information for studies of extracellular vesicles 2018 (MISEV2018): A position statement of the International Society for Extracellular Vesicles and update of the MISEV2014 guidelines. *J. Extracell. Vesicles* **7**, 1535750 (2018).
29. Foers, A. D. *et al.* Proteomic analysis of extracellular vesicles reveals an immunogenic cargo in rheumatoid arthritis synovial fluid. *Clin. Transl. Immunol.* **9**, e1185 (2020).
30. Coumans, F. A. W. *et al.* Methodological guidelines to study extracellular vesicles. *Circ. Res.* **120**, 1632–1648 (2017).
31. Gao, K. *et al.* Association between cytokines and exosomes in synovial fluid of individuals with knee osteoarthritis. *Mod. Rheumatol.* **30**, 758–764 (2020).
32. Kolhe, R. *et al.* Gender-specific differential expression of exosomal miRNA in synovial fluid of patients with osteoarthritis. *Sci. Rep.* **7**, 2029 (2017).
33. Jimenez, L. *et al.* Quantitative proteomic analysis of small and large extracellular vesicles (EVs) reveals enrichment of adhesion proteins in small EVs. *J. Proteome Res.* **18**, 947–959 (2019).
34. Johnson, S. M., Banyard, A., Smith, C., Mironov, A. & McCabe, M. G. Large extracellular vesicles can be characterised by multiplex labelling using imaging flow cytometry. *Int. J. Mol. Sci.* **21**, 8723 (2020).
35. Cloutier, N. *et al.* The exposure of autoantigens by microparticles underlies the formation of potent inflammatory components: The microparticle-associated immune complexes. *EMBO Mol. Med.* **5**, 235–249 (2013).
36. Mobarrez, F. *et al.* Microparticles in the blood of patients with SLE: Size, content of mitochondria and role in circulating immune complexes. *J. Autoimmun.* **102**, 142–149 (2019).
37. de Oliveira Jr, G. P. *et al.* Effects of endurance racing on horse plasma extracellular particle miRNA. *Equine Vet. J.* **53**, 618–627 (2021).
38. Rilla, K., Siiskonen, H., Tammi, M. & Tammi, R. Hyaluronan-coated extracellular vesicles—A novel link between hyaluronan and cancer. *Adv. Cancer Res.* **123**, 121–148 (2014).
39. Zhao, K. *et al.* Hype or hope of hyaluronic acid for osteoarthritis: Integrated clinical evidence synthesis with multi-organ transcriptomics. *J. Orthop. Transl.* **32**, 91–100 (2022).
40. Headland, S. E. *et al.* Neutrophil-derived microvesicles enter cartilage and protect the joint in inflammatory arthritis. *Sci. Transl. Med.* **7**, 315ra190 (2015).
41. Zheng, L. *et al.* Primary chondrocyte exosomes mediate osteoarthritis progression by regulating mitochondrion and immune reactivity. *Nanomedicine* **14**, 3193–3212 (2019).
42. Yin, B. *et al.* Harnessing tissue-derived extracellular vesicles for osteoarthritis theranostics. *Theranostics* **12**, 207–231 (2022).
43. Yuana, Y. *et al.* Handling and storage of human body fluids for analysis of extracellular vesicles. *J. Extracell. Vesicles* **4**, 29260 (2015).
44. Ragni, E. *et al.* Interaction with hyaluronan matrix and miRNA cargo as contributors for *in vitro* potential of mesenchymal stem cell-derived extracellular vesicles in a model of human osteoarthritic synoviocytes. *Stem Cell Res. Ther.* **10**, 109 (2019).
45. Arokoski, M. E. A., Tiitu, V., Jurvelin, J. S., Korhonen, R. K. & Fick, J. M. Topographical investigation of changes in depth-wise proteoglycan distribution in rabbit femoral articular cartilage at 4 weeks after transection of the anterior cruciate ligament. *J. Orthop. Res.* **33**, 1278–1286 (2015).
46. Jones, M., Stanish, W. & Rutherford, D. Co-activation is not altered in the contra-lateral limb of individuals with moderate knee osteoarthritis compared to healthy controls. *Clin. Biomech.* **59**, 71–77 (2018).
47. Shymkiw, R. C., Bray, R. C., Boyd, S. K., Kantzas, A. & Zernicke, R. F. Physiological and mechanical adaptation of periarticular cancellous bone after joint ligament injury. *J. Appl. Physiol.* **90**, 1083–1087 (2001).
48. Mäkelä, J. T. A. *et al.* Site-dependent changes in structure and function of lapine articular cartilage 4 weeks after anterior cruciate ligament transection. *Osteoarthr. Cartil.* **22**, 869–878 (2014).
49. Mustonen, A.-M. *et al.* Anterior cruciate ligament transection alters the n-3/n-6 fatty acid balance in the lapine infrapatellar fat pad. *Lipids Health Dis.* **18**, 67 (2019).
50. Metcalfe, A. J., Andersson, M. L. E., Goodfellow, R. & Thorstensson, C. A. Is knee osteoarthritis a symmetrical disease? Analysis of a 12 year prospective cohort study. *BMC Musculoskelet. Disord.* **13**, 153 (2012).

51. Driver, B., Marks, D. C. & van der Wal, D. E. Not all (N)SAID and done: Effects of nonsteroidal anti-inflammatory drugs and paracetamol intake on platelets. *Res. Pract. Thromb. Haemost.* **4**, 36–45 (2020).

Acknowledgements

We are thankful to the horse owners for the donation of samples for research purposes. Taija Hukkanen and Sylvain Tollis are greatly acknowledged for their technical assistance and the EV Core (University of Helsinki) for NTA. This work was carried out with the support of the Cell and Tissue Imaging Unit (University of Eastern Finland), Biocenter Kuopio, and Biocenter Finland.

Author contributions

P.N., A.-M.M., N.L., and M.R. designed and coordinated the study. N.L., M.R., and A.M. collected the samples, and N.L. and T.N. assessed the clinical macroscopic findings. T.P. conducted SF sample preparation, and P.N., A.-M.M., and K.R. performed the confocal microscopy and J.C. the image processing. S.O. performed the analyses for hyaluronan content and molecular weight distribution. P.N. conducted the statistical analyses, and P.N. and K.R. prepared the images. A.-M.M. drafted the manuscript. All authors revised the draft critically and read and approved the final submitted manuscript.

Funding

Financial support for the study was provided by the Academy of Finland (Grant #322429 to P.N.). The funding source had no involvement in the study design, in the collection, analysis, and interpretation of data, in the writing of the report, or in the decision to submit the article for publication.

Competing interests

The authors declare no competing interests.

Additional information

Correspondence and requests for materials should be addressed to A.-M.M.

Reprints and permissions information is available at www.nature.com/reprints.

Publisher's note Springer Nature remains neutral with regard to jurisdictional claims in published maps and institutional affiliations.



Open Access This article is licensed under a Creative Commons Attribution 4.0 International License, which permits use, sharing, adaptation, distribution and reproduction in any medium or format, as long as you give appropriate credit to the original author(s) and the source, provide a link to the Creative Commons licence, and indicate if changes were made. The images or other third party material in this article are included in the article's Creative Commons licence, unless indicated otherwise in a credit line to the material. If material is not included in the article's Creative Commons licence and your intended use is not permitted by statutory regulation or exceeds the permitted use, you will need to obtain permission directly from the copyright holder. To view a copy of this licence, visit <http://creativecommons.org/licenses/by/4.0/>.

© The Author(s) 2022